Local and network changes after multichannel transcranial direct current stimulation using magnetoencephalography in patients with refractory epilepsy

Maeva Daoud, Samuel Medina Villalon, Ricardo Salvador, Maria Fratello, Khoubeib Kanzari, Francesca Pizzo, Giada Damiani, Elodie Marie Garnier, Jean-Michel Badier, Fabrice Wendling, et al.

Clinical Neurophysiology 170 (2025) 145–155

Contents lists available at ScienceDirect

Clinical Neurophysiology

journal homepage: www.elsevier.com/locate/clinph

Local and network changes after multichannel transcranial direct current stimulation using magnetoencephalography in patients with refractory epilepsy

Maeva Daoud [a], Samuel Medina Villalon [b], Ricardo Salvador [c], Maria Fratello [a], Khoubeib Kanzari [a], Francesca Pizzo [b], Giada Damiani [c], Elodie Garnier [a], Jean-Michel Badier [a], Fabrice Wendling [d], Giulio Ruffini [c], Christian Bénar [a,1], Fabrice Bartolomei [b,*,1]

[a] Aix-Marseille Université, INSERM, INS, Institut de Neurosciences des Systèmes, Marseille 13005, France
[b] APHM, Timone Hospital, Epileptology and Cerebral Rhythmology, Marseille, France
[c] Neuroelectrics, Barcelona, Spain
[d] Rennes Univ, INSERM, LTSI U1099, F 35000 Rennes, France

ARTICLE INFO

Keywords:
Drug-resistant epilepsy
Multichannel tDCS
Magnetoencephalography
Source reconstruction
Functional connectivity
Power spectral density

ABSTRACT

Objective: Non-invasive neuromodulation techniques, particularly transcranial direct current stimulation (tDCS), are promising for drug-resistant epilepsy (DRE), though the mechanisms of their efficacy remain unclear. This study aims to (i) investigate tDCS neurophysiological mechanisms using a personalized multichannel protocol with magnetoencephalography (MEG) and (ii) assess post-tDCS changes in brain connectivity, correlating them with clinical outcomes.

Methods: Seventeen patients with focal DRE underwent three cycles of tDCS over five days, each consisting of 40-minute stimulations targeting the epileptogenic zone (EZ) identified via stereo-EEG. MEG was performed before and after sessions to assess functional connectivity (FC) and power spectral density (PSD),estimated at source level (beamforming).

Results: Five of fourteen patients experienced a seizure frequency reduction > 50 %. Distinct PSD changes were seen across frequency bands, with reduced FC in responders and increased connectivity in non-responders ($p < 0.05$). No significant differences were observed between EZ network and non-involved networks. Responders also had higher baseline FC, suggesting it could predict clinical response to tDCS in DRE.

Conclusions: Personalized multichannel tDCS induces neurophysiological changes associated with seizure reduction in DRE.

Significance: These results provide valuable insights into tDCS effects on epileptic brain networks, informing future clinical applications in epilepsy treatment.

1. Introduction

Transcranial direct current stimulation (tDCS) has emerged as a promising alternative in the treatment of focal drug-resistant epilepsies (DRE) (see (Hawas et al., 2024; San-juan et al., 2015; Simula et al., 2022) for exhaustive reviews). This non-invasive brain stimulation technique delivers a low electrical current to the cortex through scalp electrodes. The electric field under the anodal electrode is typically excitatory, while the field under the cathodal electrode is inhibitory (Nitsche and Paulus, 2001, 2000), a property utilized in treating epilepsy. Advanced methods, such as multichannel tDCS, which incorporates smaller electrode pairs, have emerged to target epileptogenic

Abbreviations: tDCS, Transcranial Direct Current Stimulation; DRE, Drug-resistant epilepsy; MEG, Magnetoencephalography; EEG, Electroencephalography; SEEG, Stereoelectroencephalography; FC, Functional Connectivity; PSD, Power Spectral Density; ICA, Independent component Analysis; R, Responders; NR, Non-responders; EZ, Epileptogenic Zone; VEP, Virtual Epileptic Patient; SF, Seizure Frequency; Icoh, Imaginary Coherence; ASM, Antiseizure Medication; C1, C2, C3, Cycle 1, Cycle 2, Cycle 3.

* Corresponding author at: Service d'Epileptologie et de Rythmologie cérébrale, Hôpital Timone, 264 Rue Saint-Pierre, 13005 Marseille, France.
E-mail address: fabrice.bartolomei@ap-hm.fr (F. Bartolomei).

[1] Christian-George Bénar and Fabrice Bartolomei are co-last authors.

https://doi.org/10.1016/j.clinph.2024.12.006
Accepted 7 December 2024
Available online 11 December 2024

brain regions with greater precision. These advances include enhanced targeting accuracy through the integration of biophysical modeling, offering avenues for optimization (Hannah et al., 2019; Ruffini et al., 2014).

To date, several clinical studies on tDCS have reported a decrease in the occurrence of seizures (Auvichayapat et al., 2013; Daoud et al., 2022; Fregni et al., 2006; Kaye et al., 2021; San-Juan et al., 2017; Tekturk et al., 2016). However, despite the therapeutic action of tDCS in epilepsy patients and the refinement of protocols, the underlying mechanisms driving clinical improvements remain poorly understood and are a topic of ongoing debate. Predominantly, studies using tDCS as an antiepileptic treatment have focused on changes in the count of interictal epileptiform discharges (IEDs) through electrophysiological recordings (Auvichayapat et al., 2013; Fregni et al., 2006). However, the reliability of this approach is debatable due to the inconsistent visibility of IEDs on scalp electroencephalographic (EEG) recordings and their weak correlation with seizure risk (review in (Simula et al., 2022)). Consequently, exploring alternative electrophysiological methods to quantify the effects of low electrical stimulation on the brain is warranted. Accumulating evidence from previous investigations underscores the need to characterize epilepsy as a large-scale brain network disorder (Bartolomei et al., 2017; Pittau and Vulliemoz, 2015). In particular, interictal alterations in functional connectivity within the epileptogenic network have been shown (Lagarde et al., 2018). Our group conducted a preliminary study involving a personalized multichannel tDCS protocol in ten patients suffering from DRE (Daoud et al., 2022). Clinical improvement in responsive patients was notably associated with a significant decrease in global functional connectivity (FC), as measured by standard scalp EEG. However, given that these findings were derived from sensor space analysis, potential uncertainties in interpreting brain interaction estimates arise, as a single region can give rise to widespread fields across multiple sensors.

The main objective of this study was to evaluate the changes in local (power spectral density measures) and network (functional connectivity) brain activity induced by tDCS, as measured by magnetoencephalography (MEG), and to establish correlations with clinical outcomes. We also explored whether alterations were confined to the inhibited areas or extended more broadly across the brain. Finally, we analyzed data before transcranial stimulation with the objective of identifying predictive biomarkers of the clinical response to tDCS.

2. Materials and methods

2.1. Study design

17 patients with drug-resistant epilepsy (DRE) were prospectively enrolled in this study. The protocol was approved by the national ethics committee (N°ID RCB 2020-A02861-38; NCT04782869). The inclusion criteria comprised: (1) age $\geq$ 12 years; (2) diagnosed with focal drug-resistant epilepsy that is either inoperable or has experienced failure of prior epilepsy surgery, (3) with at least four seizures per month at baseline; (4) previous SEEG conducted before inclusion, providing an adequate definition of unifocal epileptogenic zone. Clinical and demographic data are summarized in Table 1.

2.2. Multichannel tDCS sessions

After a baseline period of two months for each patient, the patients received daily stimulation with an individualized multichannel tDCS protocol (see below) for five consecutive days, referred here as a tDCS 'cycle'. The efficacy of tDCS and the duration of its beneficial effects depend on the stimulation duration, the number of repetitions, and the interval between sessions. Specifically, the break between tDCS sessions is crucial for optimizing cumulative effects and extending the inhibitory neuroplastic effects of cathodal stimulation in epilepsy (Monte-Silva et al., 2010). A recent study by Yang et al. found a significantly greater reduction in seizure frequency in patients with refractory focal epilepsy using a protocol of 2x20 minute stimulations per day with a 20-minute interval, compared to a protocol with a single 40-minute stimulation (Yang et al., 2020). Based on these findings, we used a 20-minute interval between two repeated sessions of 20 min to achieve prolonged beneficial effects of neuromodulation in patients. Thus, the daily treatment consisted of 40 min (2x20 minutes) of cathodal stimulation. Each cycle started and ended with a 1-hour MEG exam. This tDCS cycle, including MEG and daily tDCS, was repeated every two months, totaling three cycles within six months (Fig. 1.A).

The position of tDCS electrodes for each patient was personalized using an optimization process based on individual factors, including the location of the epileptogenic network and previous cortectomies or lesions (for details, see methodology in (Daoud et al., 2022)). In brief, the personalized approach involved creating individual head models from MRI scans and optimizing electrode placement using the Stimweaver algorithm (Ruffini et al., 2014). This algorithm determines the optimal electrode positions and currents to suppress the epileptogenic network, represented as a weighted target En-field map on the cortical surface, corresponding to the E-field perpendicular to the cortical surface. Negative En (En directed out of the cortical surface) hyperpolarizes pyramidal cell membranes, causing transient and potentially long-term decreases in cortical excitability (Galan-Gadea et al., 2023). A full explanation of this montage optimization algorithm is presented in (Ruffini et al., 2014). By combining the accurate target definition with the modeling of the effects of previous surgeries and implanted devices, the pipeline ensures both safe and optimized stimulation parameters (See supplemental Figure S1). The optimization minimizes the ERNI function, a weighted difference between En induced by each candidate solution and the target weight map. Currents were limited to a maximum of 1.884 mA per stimulation channel and 2.0 mA total injected current. Stimulation was administered using the Starstim8 tDCS system, with NG PiStim electrodes positioned in a neoprene cap (Neuroelectrics Barcelona). The current intensity was delivered in two 20-minute sessions separated by a 20-minute break to prolong inhibitory effects (Monte-Silva et al., 2010; Yang et al., 2020).

2.3. MEG recordings

On the first day of each cycle (prior to the first stimulation of the week), patients underwent a MEG recording to capture the electrophysiological brain state before stimulation. At the end of each tDCS cycle (on the 5th day), another MEG exam was performed for comparison with the pre-tDCS treatment recording. The MEG recordings were performed consistently at the same time of the day (in the morning) to avoid circadian rhythm bias (Aeschbach et al., 1999).

The biomagnetic signals used in this study were acquired using a 4D Neuroimaging™ 3600 whole head system equipped with 248 magnetometers operating at a sampling rate of 2034.51 Hz (4D Neuroimaging Inc., San Diego CA) (Pizzo et al., 2019). Each recording session consisted of five runs of 10 min during resting state (two runs with eyes closed). To co-register MEG recordings with patient's MRI images, three fiducial positions (nasion, left pre-auricular, and right pre-auricular) and head coil positions were determined.

2.4. Seizure frequency measures

The patients or/and their caregivers were asked to record daily the number and the type of seizures in a seizure diary starting two months before the study onset (baseline) and continuing until two months after the final multichannel tDCS stimulation cycle (V4). Changes in seizure frequency (SF) were expressed as a percentage of baseline frequency. Patients experiencing at least 50 % seizure reduction at the end of the study were categorized as 'responders' (R), while others were labeled as 'non-responders' (NR).

Table 1
Demographic data and epilepsy characteristics of the patients.

Patient	Gender	Age	Etiology	Seizure type	Number of ASM	SOZ defined by SEEG	Number of SEEG electrodes	Previous failed surgery	tDCS target	Injected Current (mA)	Desired E field in Target (V/m)	Number of tDCS electrodes
1	F	43	Schizencephalia, heterotopia, polymicrogyria	FSIA	3	Ltemporal mesial, Perisylvain deep, superficial, parietal lateral	19	Thermocoagulation, VNS	L MLa temporo-parietal	1.998	-0.5	7
2	F	31	FCD 2	FAS	1	TLE, L frontal mesial, central mesial and lateral	9	Cortectomy L premotor cortex	L pericentral	1.999	-0.5	8
3	M	42	Cavernoma	FSIA	4	L frontal mesial temporal mesial	9	No	L MLa, temporo-orbitofrontal	1.998	-0.25	7
4	M	48	Cryptogenic	FSIA	4	L Temporal mesial, left insula bilateral	13	Thermocoagulation, VNS (desactivated)	L MLa temporal	1.999	-0.034	6
5	F	50	FCD 1	FSIA FBTCS	5	R temporal mesial, parietal mesial, lateral bilateral (R>L)	13	Thermocoagulation, resective surgery	R pericentral/ parietal and posterior temporal (carrefour)	1.997	-0.5	8
6	F	23	Hippocampal sclerosis	FSIA	3	R mesio temporal	11	No	R MLa temporal	1.999	-0.014	7
7	M	32	Gliosis	EPC, focal motor seizures	4	R paracentral lobule	4	Gamma-knife, VNS	R pericental extended	1.998	-0.055	6
8	M	49	FCD 2	FSIA	5	L mesio frontal, mesio central	12	VNS	L pericental	1.999	-0.055	4
9	M	31	Cryptogenic	FSIA FAS FBTCS	2	L temporo mesial	16	No	L MLa temporal	1.998	-0.25	7
10	F	15	Cryptogenic	FAS	2	R lateral mesial frontal, central mesial lateral	15	Cortectomy, residual lesionectomy	R perisylvian and post central	1.999	-0.11	8
11	F	16	FCD 1	FAS	3	R frontal mesial lateral, central mesial lateral	13	Cortectomy R frontal	Bilat pericentral (R>L)	1.998	-0.25	8
12	F	23	Cryptogenic	FSA (motor and sensory symptoms)	2	R fronto lateral centro mesial, posterior	13	Thermocoagulation, VNS	R pericentral	1.999	-0.25	4
13	M	29	Cryptogenic	FSIA FAS FBTCS	3	L temporal mesial lateral	15	VNS	L MLa Temporal Plus dorso-lateral frontal	1.999	-0.02	8
14	M	16	Infectious/trauma, MRI left hemispheric atrophy	FAS (sensitive symptoms)	4	L frontal lateral centro lateral parietal	15	No	L carrefour and dorso-lateral pre-frontal	1.999	-0.08	7
15	F	23	Heterotopia	FAS (visual symptoms)	3	L occipito temporal mesial	10	Thermocoagulation	L occipital plus posterior baso-temporal	1.999	Lat -0.029 Mesial -0.031	6
16	F	12	Cryptogenic	EPC, focal motor seizures, FBTCS	3	Left fronto mesio lateral	8	Thermocoagulation	L pericentral	1.99	-0.216	7
17	F	30	FCD 2	FSIA FBTCS	4	L paracentral lobule	9	No	L pericentral	1.999	-0.25	8

Abbreviations: FCD: Focal Cortical Dysplasia; EPC: Epilepsia Partialis Continua; ASM: Antiseizure Medication; SOZ: Seizure Onset Zone; TLE: Temporal Lobe Epilepsy; SEEG: Stereoelectrocencephalography; VNS: Vagus Nerve Stimulation; L: Left; R: Right; MLa: Mesio-lateral. SGTC: Secondary generalized tonic-clonic seizures. FAS: focal aware seizure; FSIA: focal seizure with impaired awareness, FBTCS: focal to bilateral tonic clonic seizure.

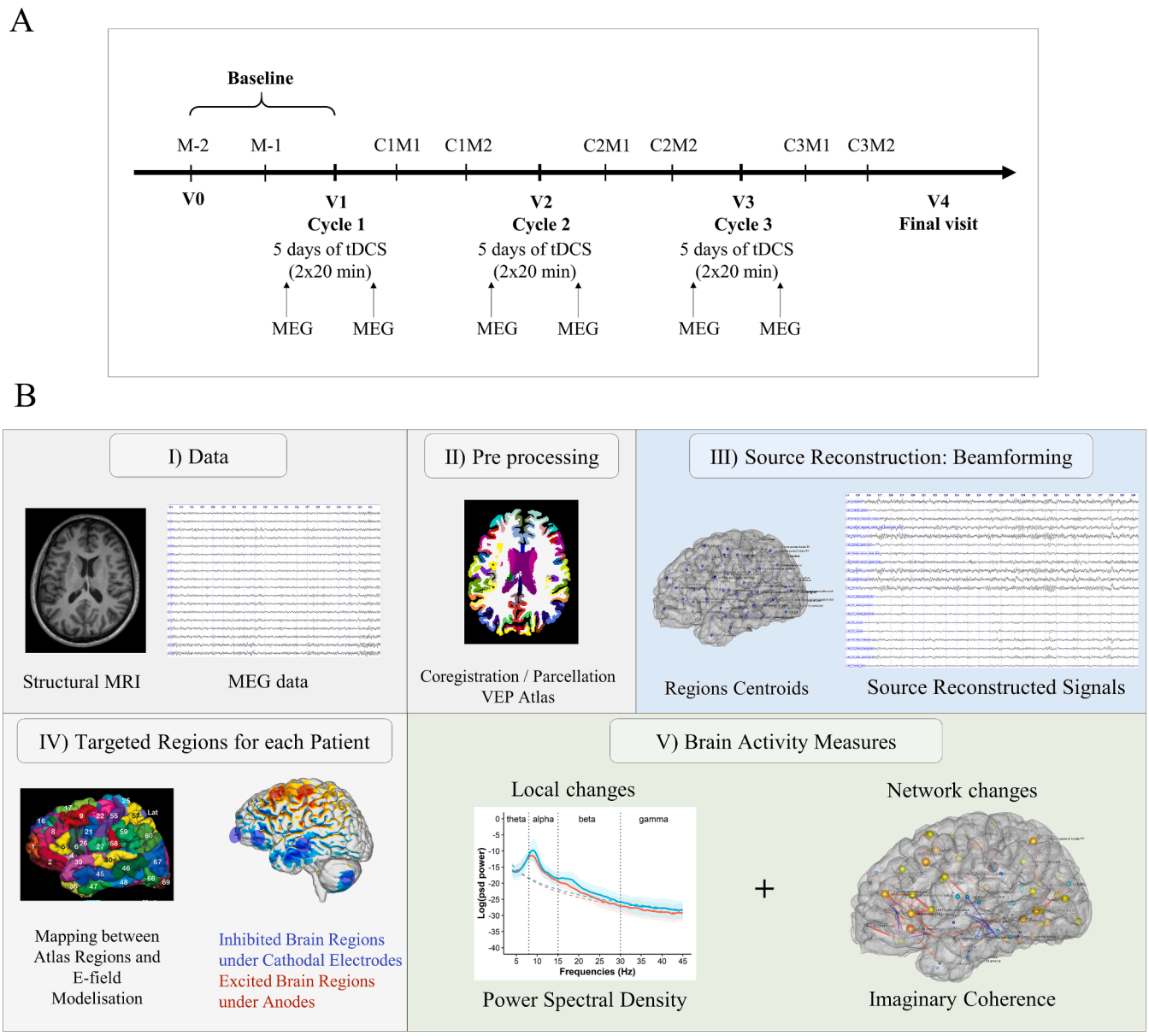

Fig. 1. Overview of study design and data analysis pipeline. A. Study timeline. Seizure diary information was collected monthly for each cycle (C1M1, C1M2, C2M1, C2M2, C3M1, C3M2). Each tDCS cycle consisted of two 20-minute stimulation periods separated by a 20-minute off period (20 min tDCS – 20 min off – 20 min tDCS), with a 1-hour MEG recording performed before the first day of stimulation and immediately after the last day of the cycle. Cycles were repeated every 2 months for three times. B. Pipeline for MEG data analysis. After cleaning the MEG recordings (I) and performing the co-registration with the patient's MRI (II), a linearly constrained minimum-variance beamformer (LCMV-BF) was used to estimate the MEG source times series at the VEP regions level (following [29]) (III). Then, we identified the patient-specific regions of interest, including inhibited brain regions in blue and excited brain regions (in red). Finally, we performed local (power spectral density) and network (functional connectivity estimated by imaginary coherence measures) source analyses before and after each tDCS cycle. We summarized them separately for inhibitory and excitatory brain regions. *Abbreviations: tDCS: Transcranial Direct Current Stimulation; MEG: Magnetoencephalography; M−2, M−1: 1 and 2 months before the first stimulation cycle (baseline period); V0: Visit 0 Inclusion; C1M1: 1 month (M1) after the first cycle (C1); C1M2: 2 months (M2) after the first cycle (C1); C2M1: 1 month (M1) after the second cycle (C2); C2M2: 2 months after the second cycle; C3M1: 1 month after the third cycle; C3M2: 2 months after the third cycle; V4: Visit 4, final visit; MRI: Magnetic Resonance Imaging; VEP: Virtual Epileptic Patient.*

2.5. MEG data pre-processing and source reconstruction

MEG data were analyzed using the AnyWave software (Colombet et al., 2015) (https://meg.univ-amu.fr/wiki/AnyWave) and Matlab in-house scripts (The Mathworks Inc., MA, USA). The MEG signals were first bandpass filtered in the range [1–70 Hz] a notch-filtered at 50 Hz. All MEG channels were thoroughly examined, and channels displaying noise or flat signals were excluded from the analysis. We additionally removed artifacts using independent component analysis (ICA) (Barbati et al., 2004), including those related to cardiac activity, muscle interference, and eye movements. Subsequently, the MEG signals were visually inspected, and any segments containing residual artifacts not identified by the ICA analysis were excluded.

Regarding the MEG source localization and reconstruction, we used the open-source FieldTrip toolbox (Oostenveld et al., 2011). The forward model was computed using OpenMEEG (Gramfort et al., 2010; Kybic et al., 2005). For the inverse solutions, we used the linearly constrained minimum-variance beamformer (LCMV-BF) (Van Veen et al., 1997). This method uses a spatial filter, linking the magnetic field measured by MEG sensors outside the brain to neural activities within

the brain. It uses the covariance of recorded signals without requiring assumptions about the number of active sources. The beamformer calculation results in a time series for each target location within the brain, representing the activity of that source. We thus estimated the source activity at the centroids of the regions defined by the Virtual Epileptic Patient atlas (VEP Atlas) (Wang et al., 2021). The analysis schema is reported in Fig. 1B.

2.6. Local and network source analysis

Using the electrical field map generated from the tDCS montage of each patient, we delineated the excited brain regions (linked to anodal electrodes) and inhibited brain regions containing cortical areas (including EZ) associated with cathodal electrodes. These patient-specific regions of interest are represented respectively in red and blue in Fig. 1.B.

First, to assess the potential local changes induced by tDCS in the targeted brain regions, we computed the power spectral density (PSD) (using Hanning windows of 2 s, overlap of 1 s) before and after each tDCS cycle. To prepare the data for statistical analysis, we calculated the mean power in specific frequency bands (theta 4–8 Hz, alpha 8–13 Hz, beta 13–30 Hz, and gamma 30–45 Hz) for each FFT iteration, normalized by the total power in the broadband range (1–45 Hz).

Second, to evaluate the impact on network activity, we investigated functional connectivity (FC) changes at the source level following each tDCS cycle. An inherent challenge in interpreting source FC analysis is the emergence of spurious coherence due to the inevitable leakage of the inverse algorithm (Schoffelen and Gross, 2009). To mitigate this issue, we opted for the imaginary coherence measure (*icoh*, (Nolte et al., 2004)). The imaginary part of coherence specifically detects synchronizations between processes that are time-lagged to each other. This approach quantifies the coupling of oscillatory phases in the activation dynamics between two brain sources, with a focus on minimizing crosstalk effects between the sources. To obtain a distribution of values for statistical analysis, we computed the metric across 15 trials, each comprising a 2-second window with a 50 % overlap. This process was repeated throughout the entire recording, excluding artifact periods. Subsequently, multiple connectivity matrices were generated for each recording and frequency band (broadband, theta, alpha, beta, gamma). To summarize connectivity information for each region and frequency band, we calculated the normalized strength of the node. This was done by summing up all the links connected to the node and then dividing this sum by the number of connected nodes.

To investigate spectral changes between post and pre-stimulation, we performed a Wilcoxon rank sum test for each region and frequency band. This test was chosen due to the non-normal distribution of the data. We used Matlab *ranksum* function to compare all PSD values (as described above) of the two periods of interest (Day 5 – Day 1 for each cycle). Similarly, to investigate FC changes between day 5 and day 1 of each cycle (Day 5 – Day 1), per region and frequency band, we performed a Wilcoxon rank sum test between all the values of node strength of the two periods.

For each measure, we kept the values of the z-statistic (called Z-value in the manuscript) to assess any differences between R and NR, between tDCS cycles, and between brain regions.

2.7. Statistical analysis

For each frequency band, Student t-tests were used to assess the changes of Z-values in local and network activity induced by tDCS across R and NR patients, tDCS cycles, and inhibited/excited brain regions. In addition, to attempt to predict favorable responses to tDCS treatment, differences in node strength values between R and NR patients at day 1 of the first cycle were also evaluated with Wilcoxon test as values were not normally distributed. All analyses were carried out using RStudio (version 4.2.2). To address multiple comparisons, we applied Bonferroni correction to the p-values. Effect sizes were computed using Cohen's d. A p-value less than 0.05 (after adjustment) was considered statistically significant.

3. Results

Seventeen patients with diverse forms of focal refractory epilepsy were enrolled between July 2021 and April 2023 (ten females, seven males; mean age 30.2; range 12–50). Three patients were excluded from the analysis pipeline. As a result, we have included a total of 14 patients in our study analysis.

3.1. Effect of tDCS on seizure frequency

At the two-month follow-up after the last tDCS cycle, nine of the fourteen patients experienced a decrease in their seizure frequency (SF) compared to the baseline (mean decrease $-46\ \% \pm 28\ \%$) (Fig. 2). Among these patients, five were considered as responder (R) patients with a SF decrease $> 50\ \%$ (mean reduction: $-66\ \% \pm 20\ \%$). Patients 10 and 13 had to stop the tDCS stimulation after cycle 2 according to the safety protocol rules (SF increase $> 100\ \%$). Overall, only mild adverse events were reported, mostly characterized by mild itching (9/14) and tingling (4/14) sensation beneath the stimulation electrodes during the first 30 s of the stimulation period.

Importantly, to ensure that antiepileptic drugs did not influence the comparison between responders and non-responders, we confirmed that there was no significant difference in the number of antiseizure medications (ASMs) between these groups (Student's *t*-test, $T(12) = 0.692$, $p = 0.502$).

3.2. Spectral activity changes after multichannel tDCS

We first focused on PSD changes occurring between day 5 and day 1 of each cycle for R and NR patients in the whole brain (Fig. 3). The results were found to vary significantly across different frequency bands (see details in supplementary table S1). In the theta band (4–8 Hz), R patients exhibited a moderate and cumulative decrease in spectral power across cycles. Conversely, NR patients displayed a substantial and cumulative increase in PSD in the theta range across cycles, with the maximum increase observed in cycle 3. When comparing spectral power between R and NR groups, a significant and large decrease was observed in R patients in cycles 2 and 3 (Fig. 3.A). Regarding changes in the alpha band (8–13 Hz) across cycles for both R and NR, a significant increase in power was observed between cycles 1 and 2. In NR patients, the observed increase in spectral power between cycles was smaller. R patients exhibited a significant increase in alpha spectral power in all cycles compared to NR patients (Fig. 3.B). In the beta band (13–30 Hz), we noted a significant cumulative large decrease across stimulation cycles in NR patients and, conversely, an increase in the last tDCS cycle in R patients. Comparing the R and NR groups, the PSD changes varied at each tDCS cycle. After C1 and C2, R had a significantly lower PSD in the beta band than the NR group. After C3, R presented a significantly larger PSD in beta band than in NR group (Fig. 3.C).

Regarding changes in PSD within the gamma band (30–45 Hz) across cycles for R patients, a small but significant increase in power was observed between the second and the last tDCS cycle. In NR patients, we observed a cumulative decrease in spectral power in the gamma range across cycles. When comparing R and NR groups across cycles, we obtained similar results to those of the beta band. After the first cycle (C1), R had a significantly lower PSD than the NR group. After the third cycle (C3), R presented a significantly larger PSD in the gamma band than the NR group (Fig. 3.D).

We then focused on PSD changes involving the specific targeted brain regions. Supplementary figure S2 depicts the changes in PSD focusing on targeted and non-targeted regions in all frequency bands (theta, alpha, beta, gamma). We did not find significant differences in

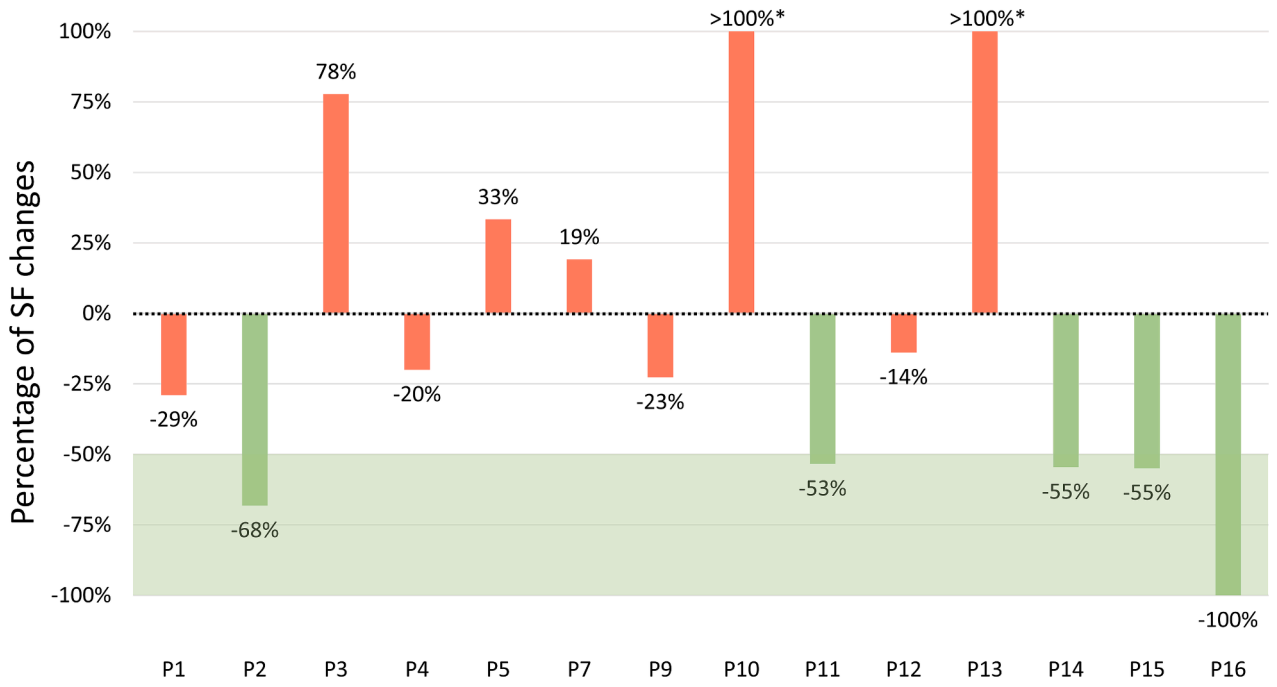

Fig. 2. Percentage change in seizure frequency compared to baseline after three tDCS cycles at the two-months follow-up (n = 14 patients). *Patients 10 and 13 had to stop the study after the cycle 2 according to the safety rules of our protocol (increase in SF > 100 %).

PSD changes between excited and inhibited brain regions.

3.3. Functional connectivity changes after multichannel tDCS

First, to gain a broader overview of potential functional changes, we examined global variations in FC by comparing node strength values of all regions between cycles and between R and NR groups (Fig. 4). The statistical results are summarized in supplemental table S2. The overall FC change pattern observed between groups and cycles appears similar across the frequency bands studied. In the broadband range (Fig. 4.A), R patients exhibited a global decrease in FC from the second cycle of stimulation. In contrast, the NR group showed either no modification or very slight changes in FC. The comparison of FC changes occurring after cycles 2 and 3 confirmed a significant decrease in FC for R compared to the NR group.

Sub-band analysis revealed that in the theta band (Fig. 4.B), we also observed a cumulative, significant decrease in FC across all brain regions in R patients between cycles. In contrast, NR patients showed a slight increase in FC across cycles. When comparing FC changes between R and NR groups, R patients presented a significant decrease in FC compared to the NR group at the second and the last tDCS cycles. The findings for other frequency bands are detailed in supplementary figure S3 and supplementary table S2.

A significant reduction in FC in the broadband range within targeted inhibited and excited brain regions was observed after cycle 2 for R patients compared to NR patients (Inhibited regions in Cycle 2, R vs NR: $t(110) = -5.0422$, $p < 0.0001$, Cohen's $d = -0.85$ [-1.19 – −0.51]; Excited regions in Cycle 2, R vs NR: $t(99) = -3.8912$, $p < 0.001$, Cohen's $d = -0.75$ [-1.15 – −0.36]) (Fig. 4.C). A similar trend was noted for the last tDCS cycle. We then analyzed whether FC changes were different in inhibited (targeted) and excited regions, and no difference was observed.

We also estimated these changes in frequency sub-bands. Fig. 4.D displays as an example the findings related to theta band. We observed a similar trend with a reduction in FC within both inhibited and excited brain regions after C2 and C3 for R patients compared to NR patients (Inhibited regions in Cycle 2, R vs NR: $t(86) = -3.3525$, $p = 0.028$, Cohen's $d = -0.62$ [-0.95 – −0.28]; Inhibited regions in Cycle 3, R vs NR: $t(105) = -4.2953$, $p < 0.001$, Cohen's $d = -0.79$ [-1.19 – −0.39]; Excited regions in Cycle 3, R vs NR: $t(79) = -4.6473p < 0.001$, Cohen's $d = -1.03$ [-1.49 – −0.56]). Finally, no significant variations between inhibited and excited regions were observed in other frequency bands (supplementary figure S3).

3.4. Pre-stimulation brain network and relationship with therapeutic outcome

We further investigated whether responders and non-responders had different properties in their brain networks before starting tDCS, potentially serving as predictors of the future response to tDCS. We used the node strength calculated from the initial MEG recording of the study— before the first stimulation in cycle 1. We found a higher global FC in the broadband range in R patients compared to NR patients before any tDCS stimulation ($W = 600{,}165$, $p < 0.0001$, Cohen's $d = 0.55$ [0.45 – 0.64]) (Fig. 5).

5. Discussion

5.1. Multichannel tDCS induced changes in spectral power according to the clinical response

Following previous studies (Daoud et al., 2022; Kaye et al., 2021), we used a personalized multichannel tDCS protocol guided by an SEEG-based definition of the target. This allowed us to optimize current levels with the expectation that the induced electric fields would maximize inhibitory stimulation at the target site (Ruffini et al., 2014). Among the 14 patients, nine disclosed a seizure decrease after the three tDCS cycles and five were classified as responders (R), with a substantial mean SF decrease of −66 % ± 20 %. MEG provided key advantages in this study by enabling precise source reconstruction and accurate localization of epileptiform disturbances with high temporal and spatial resolution (Gavaret et al., 2016) Compared to EEG, MEG minimizes volume conduction effects, enhancing source localization, particularly in deep cortical regions (Barkley and Baumgartner, 2003). This capability was essential for assessing spectral power and functional connectivity changes at the source level. Examining power spectral changes

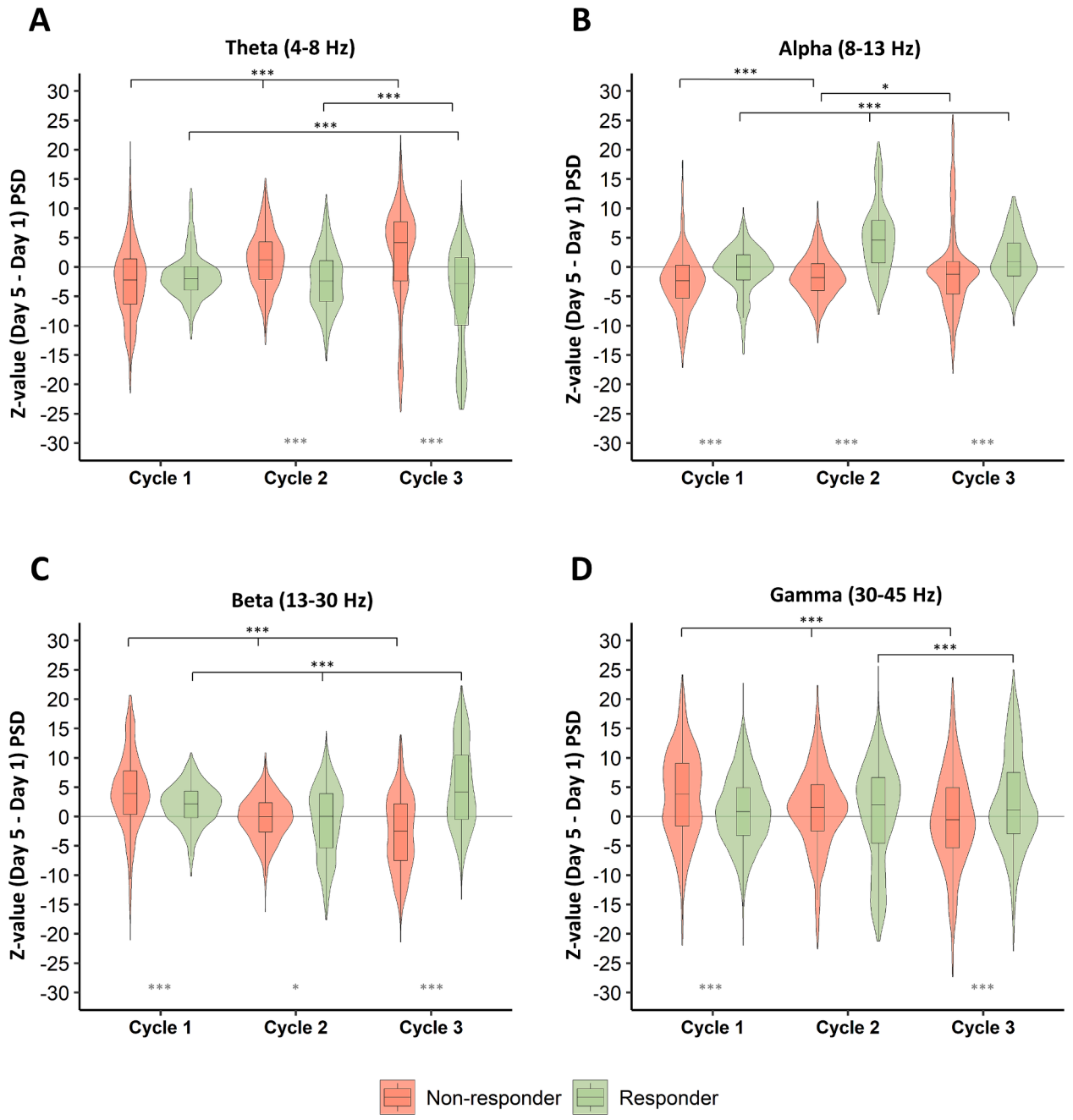

Fig. 3. Power spectral density (PSD) changes after each tDCS cycle in responder and non-responder patients. A. Violin plots represent the power spectral density (PSD) induced changes after each tDCS cycle in all brain regions in responders (in green) and non-responders (in orange) in theta band (4–8 Hz). B. In alpha band (8–13 Hz). C. In beta band (13–30 Hz). D. In gamma band (30–45 Hz). Grey asterisks represent differences between responder and non-responder groups. P-values were corrected using Bonferroni correction and black bars with asterisks representing significant differences between PSD changes occurring in cycles (* $p < 0.01$, ** $p < 0.001$, *** $p < 0.0001$).

at the source level, we found distinct patterns for the R and NR groups across different frequency bands following tDCS cycles.

Our findings indicate a cumulative decrease in spectral power in the theta band for R patients while NR patients displayed an inverse trend, with a significant increase, particularly after the third tDCS cycle. Previous studies identified an increased theta power in the interictal waking state of patients with partial and generalized epilepsy, exhibiting a consistent distribution across all derivations in EEG signals (Clemens, 2004; Douw et al., 2010). At the same time, the clinical efficacy of antiepileptic interventions, including pharmacological treatments, has been demonstrated to reduce and restore this abnormal increase in theta activity (Biondi et al., 2022). Additionally, our results indicated enhanced alpha band activity in R compared to NR patients after tDCS cycles. This observation aligns with a recent study (Ghin et al., 2021) who reported amplified EEG PSD in the alpha band using high-frequency transcranial random noise stimulation (hf-RNS) in healthy subjects. The increase in alpha activity in R patients could play an inhibitory role, consequently reducing the occurrence of seizures. The rise in signal amplitude within the alpha band is commonly linked to cortical deactivation, and inhibition, reducing cortical excitability (Klimesch et al., 2007; Romei et al., 2008; Sauseng et al., 2009). In epilepsy patients, several studies have shown a decrease in peak frequency and reduced power in the alpha band in epileptic patients, reflecting inadequate control over seizure occurrence (Abela et al., 2019; Díaz et al., 1998;

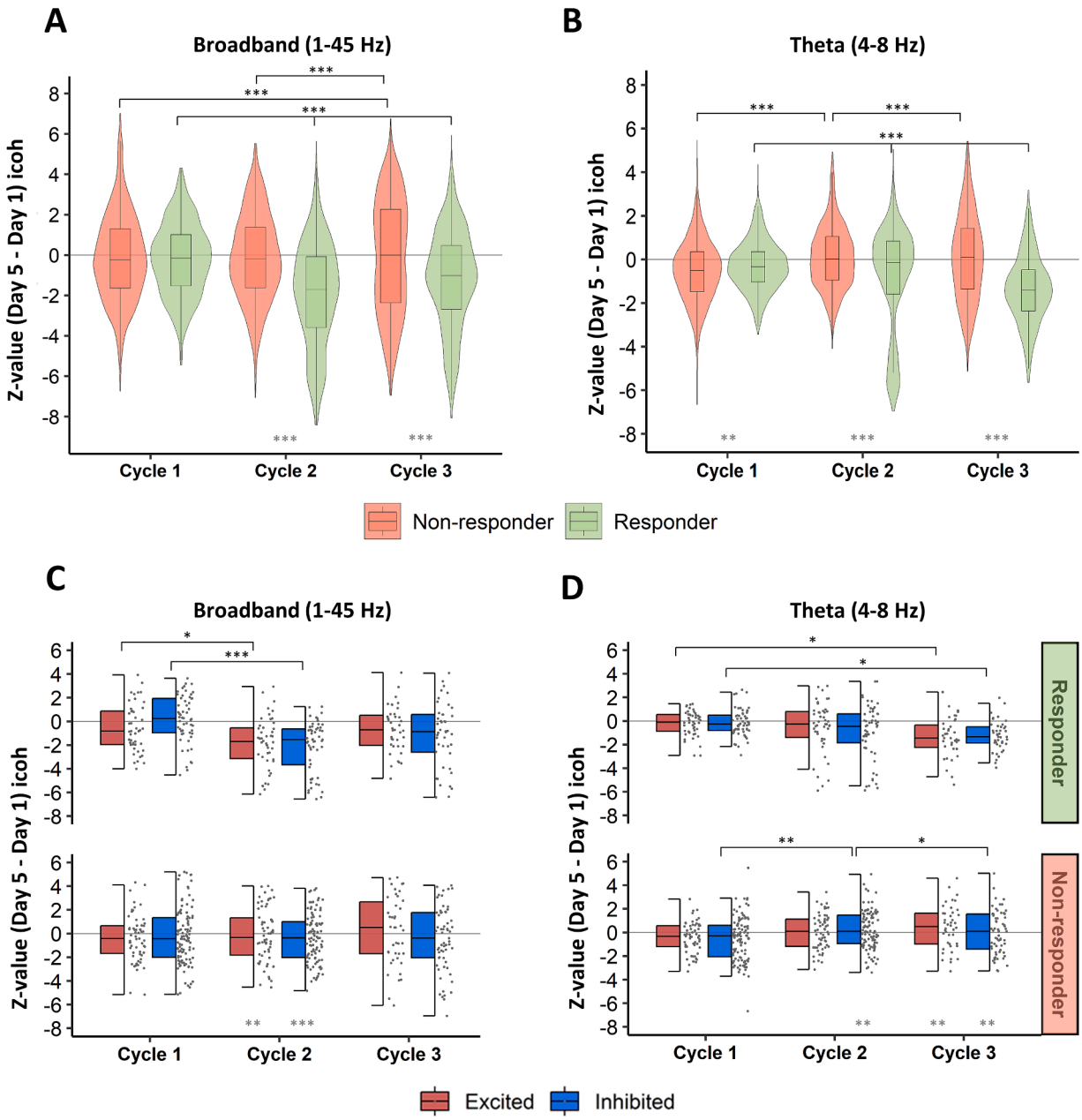

Fig. 4. Functional connectivity (FC) changes in responder and non-responder patients. In panels A and B, violin plots represent FC changes after each tDCS cycle in all brain regions at source level in responder (in green) and non-responder patients (in orange) in broadband (A) and in theta band (B). In panels C and D, half-boxplots illustrate FC-induced changes in broadband (C) and in theta band (D) after each tDCS cycle within inhibited brain regions (under cathodal tDCS electrodes in blue) and within excited brain regions (under anodal tDCS electrodes in red) for responder and non-responder patients. Each data point represents the z-value of one source region (zero: no FC change after the tDCS cycle; negative/positive z-value: decrease/increase of FC after the tDCS cycle). Grey asterisks represent differences between responder and non-responder groups. P-values were corrected using Bonferroni correction, and black bars with asterisks represent the differences between FC changes occurring in cycles (* $p < 0.01$, ** $p < 0.001$, *** $p < 0.0001$).

Larsson and Kostov, 2005).

We also observed that the spectral modifications induced by tDCS in the beta band differed between R and NR across stimulation cycles. R patients tended to have an increase in beta band power with successive cycles, whereas NR showed a power decrease. In line with the fluctuations observed during stimulation cycles, epilepsy studies examining the spectral features of the beta band have yielded contradictory outcomes. Some studies emphasized the inhibitory role of beta activity (Pellegrino et al., 2021), highlighting heightened oscillatory activity in response to specific antiepileptic drugs (Cho et al., 2012; Marrosu et al., 2005). Conversely, other research revealed an abnormal increase in beta band power in epilepsy patients (Miyauchi et al., 1991; Pegg et al., 2020), suggesting reduced beta activity following deep brain stimulation (DBS) as a potential clinical efficacy biomarker (Tong et al., 2022).

Interestingly, no significant differences were observed when comparing PSD changes between excited and inhibited brain regions within the same patient group across all frequency bands. This suggests that the spectral content was altered uniformly throughout the entire brain and not specifically within the inhibited targeted regions, i.e., the areas around the epileptogenic zone. Another investigation using a high-definition protocol of responsive neurostimulation (hf-RNS) similarly reported this widespread phenomenon (Ghin et al., 2021).

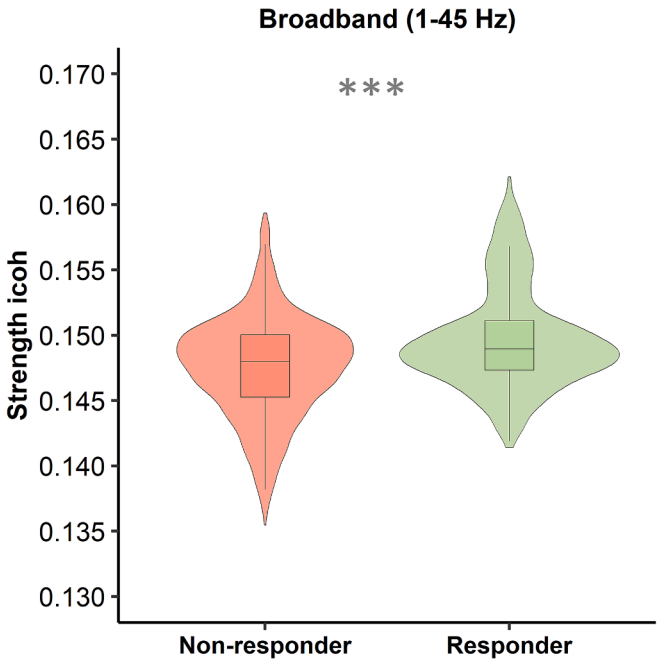

Fig. 5. Functional connectivity measured before the first tDCS stimulation in responder and non-responder patients. The data represented by violin plots corresponds to the node strength changes in all source regions for the patients of each group (R vs NR). Grey asterisks represent differences between responder and non-responder groups (*** $p < 0.0001$).

5.2. Multichannel tDCS induces whole brain functional changes based on clinical response

Previous research has shown that heightened connectivity is observed in both the epileptogenic zone and the propagation zone when compared to the non-involved zone (NIZ)(Bartolomei et al., 2017; Lagarde et al., 2022). It is reasonable to hypothesize that effective antiepileptic therapy could normalize functional connectivity, as it has already been shown in VNS (Bodin et al., 2015; Sangare et al., 2020), thalamic stimulation (Deutschová et al., 2021; Scherer et al., 2020), or after SEEG radiofrequency ablation (Simula et al., 2023). To date, several recent studies have suggested an association between a tDCS-induced decrease in FC or in synchronization induced by tDCS and its clinical effectiveness, measured by seizure frequency reduction (Daoud et al., 2022; Lin et al., 2018; Luo et al., 2021). However, the connectivity estimations in these studies were elementary, derived from simple scalp EEG with only a few channels. Our study showed that R patients, after the second and the third tDCS cycles, exhibited a decrease in overall source level-functional connectivity compared to NR across all frequency bands. Additionally, no significant differences were observed when comparing functional changes in brain regions involved in the epileptogenic zone (under cathodes) to non-involved regions (under anodes). This is consistent with the PSD results and supports the assumption that, despite being a focal method, tDCS exerts a widespread and robust influence on the whole brain networks. Previous research suggested the possibility of inducing effects affecting both local and network-to-network connectivity dynamics when applying multi-channel tDCS in healthy subjects (Mencarelli et al., 2020; Ruffini et al., 2018).

5.3. Functional source connectivity as a predictive biomarker for clinical response to tDCS?

We finally observed that individuals who later showed a positive clinical response to tDCS had a baseline FC level significantly higher than the FC level observed in NR patients, prior to the start of the first tDCS stimulation. The state of the brain networks before the start of the therapeutic procedure could be predictive of the treatment response. This has already been suggested with other types of neurostimulation. Before treatment with VNS, it has been shown that the network topology measured by MEG was different in R and NR patients (Babajani-Feremi et al., 2018). A higher pre-intervention level of functional connectivity has also been found in patients responding to pulvinar-DBS compared to NR patients (Deutschová et al., 2021). In a trial aimed at predicting the treatment outcome of cathodal tDCS in focal epilepsy, Hao and colleagues used graph theoretical analysis based on fMRI data (Hao et al., 2021). By employing a support vector machine (SVM) prediction model, they achieved a promising mean accuracy of 68.3 %, demonstrating the potential for clinical prediction of tDCS treatment outcomes in epilepsy patients.

5.4. Limitations

The first limitation is related to the small sample size, so further studies should adopt a multicentric approach to enhance patient enrollment. Secondly, the absence of a sham control group in our study raises concerns about the robustness of the findings. However, earlier tDCS investigations have shown a notable placebo response of approximately 13–27 % change in seizure frequency [66]. When assessing responder patients exhibiting a reduction in seizure frequency exceeding 50 %, our findings surpass this range significantly. Moreover, the lack of a sham control group opens the possibility that non specific factors, such as variations in attention or alertness, may have influenced the observed outcomes. While comparisons between responders and non-responders suggest these differences are unlikely to fully explain the differences, further research with sham-controlled designs is essential to assess the specific effects of tDCS definitively. Thirdly, although antiepileptic drugs were consistent across all patients during treatment and follow-up, and no differences were found in the total number of ASMs between responders and non-responders, there was variability in the types of medications used. This variability might have influenced the efficacy of tDCS and the observed changes in PSD and functional connectivity.

6. Conclusion

The acquisition of MEG data before and after multiple cycles of multichannel tDCS, coupled with source reconstruction analysis, enabled the identification of induced changes in power spectral density and in functional connectivity in whole brain networks. Notably, distinct patterns of brain changes were observed between responder and non-responder patients. The findings pave the way for future investigations, offering potential clinical applications and enhancing our understanding of tDCS effects on epileptic brain networks.

Funding

This work is supported by the European Research Council: Galvani project, ERC-SyG 2019, grant agreement No 855109. This work was performed on a platform member of France Life Imaging network (ANR-11-INBS-0006).

Declaration of Competing Interest

The authors declare the following financial interests/personal relationships which may be considered as potential competing interests: The non-invasive brain stimulation device used in this study was produced by Neuroelectrics Corp. and Starlab Neuroscience. Dr. Giulio Ruffini is a co-founder of these companies, Dr. Ricardo Salvador and Dr Giada Damiani work for this company. All the other authors state there is no conflict of interest.

Acknowledgments

This work is supported by the European Research Council: Galvani project, ERC-SyG 2019, grant agreement No 855109. This work was performed on a platform member of France Life Imaging network (grant ANR-11-INBS-0006).

We acknowledge Mégane Delourme, Pauline Rontani and Sophie Tardoski-Leblanc, members of Research direction of APHM (Assistance Publique des Hôpitaux de Marseille) for their administrative contribution which enabled the successful completion of this project.

We thank Bruno Colombet for his technical assistance. We extend our thanks to all the patients who consented to participate in this study, as well as to the clinical staff for their support.

Appendix A. Supplementary data

Supplementary data to this article can be found online at https://doi.org/10.1016/j.clinph.2024.12.006.

References

Abela, E., Pawley, A.D., Tangwiriyasakul, C., Yaakub, S.N., Chowdhury, F.A., Elwes, R.D. C., et al., 2019. Slower alpha rhythm associates with poorer seizure control in epilepsy. Ann. Clin. Transl. Neurol. 6, 333–343. https://doi.org/10.1002/acn3.710.

Aeschbach, D., Matthews, J.R., Postolache, T.T., Jackson, M.A., Giesen, H.A., Wehr, T.A., 1999. Two circadian rhythms in the human electroencephalogram during wakefulness. Am. J. Physiol. Regul., Integr. Compar. Physiol. 277, R1771–R1779. https://doi.org/10.1152/ajpregu.1999.277.6.R1771.

Auvichayapat, N., Rotenberg, A., Gersner, R., Ngodklang, S., Tiamkao, S., Tassaneeyakul, W., et al., 2013. Transcranial direct current stimulation for treatment of refractory childhood focal epilepsy. Brain Stimul. 6, 696–700. https://doi.org/10.1016/j.brs.2013.01.009.

Babajani-Feremi, A., Noorizadeh, N., Mudigoudar, B., Wheless, J.W., 2018. Predicting seizure outcome of vagus nerve stimulation using MEG-based network topology. Neuroimage Clin 19, 990–999. https://doi.org/10.1016/j.nicl.2018.06.017.

Barbati, G., Porcaro, C., Zappasodi, F., Rossini, P.M., Tecchio, F., 2004. Optimization of an independent component analysis approach for artifact identification and removal in magnetoencephalographic signals. Clin. Neurophysiol. 115, 1220–1232. https://doi.org/10.1016/j.clinph.2003.12.015.

Barkley, G.L., Baumgartner, C., 2003. MEG and EEG in Epilepsy. J. Clin. Neurophysiol. 20, 163–178. https://doi.org/10.1097/00004691-200305000-00002.

Bartolomei, F., Lagarde, S., Wendling, F., McGonigal, A., Jirsa, V., Guye, M., et al., 2017. Defining epileptogenic networks: Contribution of SEEG and signal analysis. Epilepsia 58, 1131–1147. https://doi.org/10.1111/epi.13791.

Biondi, A., Rocchi, L., Santoro, V., Rossini, P.G., Beatch, G.N., Richardson, M.P., et al., 2022. Spontaneous and TMS-related EEG changes as new biomarkers to measure anti-epileptic drug effects. Sci Rep 12, 1919. https://doi.org/10.1038/s41598-022-05179-x.

Bodin, C., Aubert, S., Daquin, G., Carron, R., Scavarda, D., McGonigal, A., et al., 2015. Responders to vagus nerve stimulation (VNS) in refractory epilepsy have reduced interictal cortical synchronicity on scalp EEG. Epilepsy Res 113, 98–103. https://doi.org/10.1016/j.eplepsyres.2015.03.018.

Cho, J.R., Koo, D.L., Joo, E.Y., Yoon, S.M., Ju, E., Lee, J., et al., 2012. Effect of levetiracetam monotherapy on background EEG activity and cognition in drug-naïve epilepsy patients. Clin. Neurophysiol. 123, 883–891. https://doi.org/10.1016/j.clinph.2011.09.012.

Clemens, B., 2004. Pathological theta oscillations in idiopathic generalised epilepsy. Clin. Neurophysiol. 115, 1436–1441. https://doi.org/10.1016/j.clinph.2004.01.018.

Colombet, B., Woodman, M., Badier, J.M., Bénar, C.G., 2015. AnyWave: A cross-platform and modular software for visualizing and processing electrophysiological signals. J Neurosci Methods 242, 118–126. https://doi.org/10.1016/j.jneumeth.2015.01.017.

Daoud, M., Salvador, R., El Youssef, N., Fierain, A., Garnier, E., Biagi, M.C., et al., 2022. Stereo-EEG based personalized multichannel transcranial direct current stimulation in drug-resistant epilepsy. Clin. Neurophysiol. 137, 142–151. https://doi.org/10.1016/j.clinph.2022.02.023.

Deutschová, B., Pizzo, F., Giusiano, B., Villalon, S.M., Carron, R., Bénar, C., et al., 2021. Ictal connectivity changes induced by pulvinar stimulation correlate with improvement of awareness. Brain Stimul 14, 344–346. https://doi.org/10.1016/j.brs.2021.01.021.

Díaz GF, Virués T, San Martín M, Ruiz M, Galán L, Paz L, et al. Generalized background qEEG abnormalities in localized symptomatic epilepsy. Electroencephalogr Clin Neurophysiol 1998;106:501–7. https://doi.org/10.1016/S0013-4694(98)00026-1.

Douw, L., de Groot, M., van Dellen, E., Heimans, J.J., Ronner, H.E., Stam, C.J., et al., 2010. 'Functional Connectivity' Is a Sensitive Predictor of Epilepsy Diagnosis after the First Seizure. PLoS One 5, e10839. https://doi.org/10.1371/journal.pone.0010839.

Fregni, F., Thome-Souza, S., Nitsche, M.A., Freedman, S.D., Valente, K.D., Pascual-Leone, A., 2006. A Controlled Clinical Trial of Cathodal DC Polarization in Patients with Refractory Epilepsy. Epilepsia 47, 335–342. https://doi.org/10.1111/j.1528-1167.2006.00426.x.

Galan-Gadea, A., Salvador, R., Bartolomei, F., Wendling, F., Ruffini, G., 2023. Spherical harmonics representation of the steady-state membrane potential shift induced by tDCS in realistic neuron models. J Neural Eng 20, 026004. https://doi.org/10.1088/1741-2552/acbabd.

Gavaret, M., Dubarry, A.-S., Carron, R., Bartolomei, F., Trébuchon, A., Bénar, C.-G., 2016. Simultaneous SEEG-MEG-EEG recordings Overcome the SEEG limited spatial sampling. Epilepsy Res 128, 68–72. https://doi.org/10.1016/j.eplepsyres.2016.10.013.

Ghin, F., O'Hare, L., Pavan, A., 2021. Electrophysiological aftereffects of high-frequency transcranial random noise stimulation (hf-tRNS): an EEG investigation. Exp Brain Res 239, 2399–2418. https://doi.org/10.1007/s00221-021-06142-4.

Gramfort, A., Papadopoulo, T., Olivi, E., Clerc, M., 2010. OpenMEEG: opensource software for quasistatic bioelectromagnetics. Biomed Eng Online 9, 45. https://doi.org/10.1186/1475-925X-9-45.

Hannah, R., Iacovou, A., Rothwell, J.C., 2019. Direction of TDCS current flow in human sensorimotor cortex influences behavioural learning. Brain Stimul 12, 684–692. https://doi.org/10.1016/j.brs.2019.01.016.

Hao J, Luo W, Xie Y, Feng Y, Sun W, Peng W, et al. Functional Network Alterations as Markers for Predicting the Treatment Outcome of Cathodal Transcranial Direct Current Stimulation in Focal Epilepsy. Front Hum Neurosci 2021;15. https://doi.org/10.3389/fnhum.2021.637071.

Hawas Y, Alkhawaldeh I, Alsalhi H, Matin R, Ibrahim G, Negida A. Transcranial Direct Current Stimulation (tDCS) in Treatment of Refractory Epilepsy: A Systematic Review and Meta-analysis (P3-1.011). Neurology 2024;102. https://doi.org/10.1212/WNL.0000000000206380.

Kaye, H.L., San-Juan, D., Salvador, R., Biagi, M.C., Dubreuil-Vall, L., Damar, U., et al., 2021. Personalized, Multisession, Multichannel Transcranial Direct Current Stimulation in Medication-Refractory Focal Epilepsy: An Open-Label Study. J Clin Neurophysiol. https://doi.org/10.1097/WNP.0000000000000838.

Klimesch, W., Sauseng, P., Hanslmayr, S., 2007. EEG alpha oscillations: The inhibition–timing hypothesis. Brain Res Rev 53, 63–88. https://doi.org/10.1016/j.brainresrev.2006.06.003.

Kybic, J., Clerc, M., Abboud, T., Faugeras, O., Keriven, R., Papadopoulo, T., 2005. A common formalism for the Integral formulations of the forward EEG problem. IEEE Trans Med Imaging 24, 12–28. https://doi.org/10.1109/TMI.2004.837363.

Lagarde, S., Roehri, N., Lambert, I., Trebuchon, A., McGonigal, A., Carron, R., et al., 2018. Interictal stereotactic-EEG functional connectivity in refractory focal epilepsies. Brain 141, 2966–2980. https://doi.org/10.1093/brain/awy214.

Lagarde, S., Bénar, C.-G., Wendling, F., Bartolomei, F., 2022. Interictal Functional Connectivity in Focal Refractory Epilepsies Investigated by Intracranial EEG. Brain Connect 12, 850–869. https://doi.org/10.1089/brain.2021.0190.

Larsson, P., Kostov, H., 2005. Lower frequency variability in the alpha activity in EEG among patients with epilepsy. Clin. Neurophysiol. 116, 2701–2706. https://doi.org/10.1016/j.clinph.2005.07.019.

Lin, L.-C., Ouyang, C.-S., Chiang, C.-T., Yang, R.-C., Wu, R.-C., Wu, H.-C., 2018. Cumulative effect of transcranial direct current stimulation in patients with partial refractory epilepsy and its association with phase lag index-A preliminary study. Epilepsy Behav. 84, 142–147. https://doi.org/10.1016/j.yebeh.2018.04.017.

Luo, W.-Y., Liu, H., Feng, Y., Hao, J.-X., Zhang, Y.-J., Peng, W.-F., et al., 2021. Efficacy of cathodal transcranial direct current stimulation on electroencephalographic functional networks in patients with focal epilepsy: Preliminary findings. Epilepsy Res 178, 106791. https://doi.org/10.1016/j.eplepsyres.2021.106791.

Marrosu, F., Santoni, F., Puligheddu, M., Barberini, L., Maleci, A., Ennas, F., et al., 2005. Increase in 20–50Hz (gamma frequencies) power spectrum and synchronization after chronic vagal nerve stimulation. Clin. Neurophysiol. 116, 2026–2036. https://doi.org/10.1016/j.clinph.2005.06.015.

Mencarelli, L., Menardi, A., Neri, F., Monti, L., Ruffini, G., Salvador, R., et al., 2020. Impact of network-targeted multichannel transcranial direct current stimulation on intrinsic and network-to-network functional connectivity. J Neurosci Res 98, 1843–1856. https://doi.org/10.1002/jnr.24690.

Miyauchi, T., Endo, K., Yamaguchi, T., Hagimoto, H., 1991. Computerized Analysis of EEG Background Activity in Epileptic Patients. Epilepsia 32, 870–881. https://doi.org/10.1111/j.1528-1157.1991.tb05544.x.

Monte-Silva, K., Kuo, M.-F., Liebetanz, D., Paulus, W., Nitsche, M.A., 2010. Shaping the Optimal Repetition Interval for Cathodal Transcranial Direct Current Stimulation (tDCS). J Neurophysiol 103, 1735–1740. https://doi.org/10.1152/jn.00924.2009.

Nitsche, M.A., Paulus, W., 2000. Excitability changes induced in the human motor cortex by weak transcranial direct current stimulation. J Physiol 527, 633–639. https://doi.org/10.1111/j.1469-7793.2000.t01-1-00633.x.

Nitsche, M.A., Paulus, W., 2001. Sustained excitability elevations induced by transcranial DC motor cortex stimulation in humans. Neurology 57, 1899–1901. https://doi.org/10.1212/WNL.57.10.1899.

Nolte, G., Bai, O., Wheaton, L., Mari, Z., Vorbach, S., Hallett, M., 2004. Identifying true brain interaction from EEG data using the imaginary part of coherency. Clin. Neurophysiol. 115, 2292–2307. https://doi.org/10.1016/j.clinph.2004.04.029.

Oostenveld, R., Fries, P., Maris, E., Schoffelen, J.-M., 2011. FieldTrip: Open Source Software for Advanced Analysis of MEG, EEG, and Invasive Electrophysiological Data. Comput Intell Neurosci 2011, 1–9. https://doi.org/10.1155/2011/156869.

Pegg, E.J., Taylor, J.R., Mohanraj, R., 2020. Spectral power of interictal EEG in the diagnosis and prognosis of idiopathic generalized epilepsies. Epilepsy Behav. 112, 107427. https://doi.org/10.1016/j.yebeh.2020.107427.

Pellegrino, G., Hedrich, T., Sziklas, V., Lina, J., Grova, C., Kobayashi, E., 2021. How cerebral cortex protects itself from interictal spikes: The alpha/beta inhibition mechanism. Hum Brain Mapp 42, 3352–3365. https://doi.org/10.1002/hbm.25422.

Pittau, F., Vulliemoz, S., 2015. Functional brain networks in epilepsy. Curr Opin Neurol 28, 338–343. https://doi.org/10.1097/WCO.0000000000000221.

Pizzo, F., Roehri, N., Medina Villalon, S., Trébuchon, A., Chen, S., Lagarde, S., et al., 2019. Deep brain activities can be detected with magnetoencephalography. Nat Commun 10, 971. https://doi.org/10.1038/s41467-019-08665-5.

Romei, V., Brodbeck, V., Michel, C., Amedi, A., Pascual-Leone, A., Thut, G., 2008. Spontaneous Fluctuations in Posterior -Band EEG Activity Reflect Variability in Excitability of Human Visual Areas. Cereb. Cortex 18, 2010–2018. https://doi.org/10.1093/cercor/bhm229.

Ruffini, G., Fox, M.D., Ripolles, O., Miranda, P.C., Pascual-Leone, A., 2014. Optimization of multifocal transcranial current stimulation for weighted cortical pattern targeting from realistic modeling of electric fields. Neuroimage 89, 216–225. https://doi.org/10.1016/j.neuroimage.2013.12.002.

Ruffini, G., Wendling, F., Sanchez-Todo, R., Santarnecchi, E., 2018. Targeting brain networks with multichannel transcranial current stimulation (tCS). Curr Opin Biomed Eng 8, 70–77. https://doi.org/10.1016/j.cobme.2018.11.001.

Sangare, A., Marchi, A., Pruvost-Robieux, E., Soufflet, C., Crepon, B., Ramdani, C., et al., 2020. The Effectiveness of Vagus Nerve Stimulation in Drug-Resistant Epilepsy Correlates with Vagus Nerve Stimulation-Induced Electroencephalography Desynchronization. Brain Connect 10, 566–577. https://doi.org/10.1089/brain.2020.0798.

San-juan, D., Morales-Quezada, L., Orozco Garduño, A.J., Alonso-Vanegas, M., González-Aragón, M.F., Espinoza López, D.A., et al., 2015. Transcranial Direct Current Stimulation in Epilepsy. Brain Stimul 8, 455–464. https://doi.org/10.1016/j.brs.2015.01.001.

San-Juan, D., Espinoza López, D.A., Vázquez Gregorio, R., Trenado, C., Fernández-González Aragón, M., Morales-Quezada, L., et al., 2017. Transcranial Direct Current Stimulation in Mesial Temporal Lobe Epilepsy and Hippocampal Sclerosis. Brain Stimul 10, 28–35. https://doi.org/10.1016/j.brs.2016.08.013.

Sauseng, P., Klimesch, W., Gerloff, C., Hummel, F.C., 2009. Spontaneous locally restricted EEG alpha activity determines cortical excitability in the motor cortex. Neuropsychologia 47, 284–288. https://doi.org/10.1016/j.neuropsychologia.2008.07.021.

Scherer, M., Milosevic, L., Guggenberger, R., Maus, V., Naros, G., Grimm, F., et al., 2020. Desynchronization of temporal lobe theta-band activity during effective anterior thalamus deep brain stimulation in epilepsy. Neuroimage 218, 116967. https://doi.org/10.1016/j.neuroimage.2020.116967.

Schoffelen, J., Gross, J., 2009. Source connectivity analysis with MEG and EEG. Hum Brain Mapp 30, 1857–1865. https://doi.org/10.1002/hbm.20745.

Simula, S., Daoud, M., Ruffini, G., Biagi, M.C., Bénar, C.-G., Benquet, P., et al., 2022. Transcranial current stimulation in epilepsy: A systematic review of the fundamental and clinical aspects. Front Neurosci 16. https://doi.org/10.3389/fnins.2022.909421.

Simula, S., Garnier, E., Contento, M., Pizzo, F., Makhalova, J., Lagarde, S., et al., 2023. Changes in local and network brain activity after stereotactic thermocoagulation in patients with <scp>drug-resistant</scp> epilepsy. Epilepsia 64, 1582–1593. https://doi.org/10.1111/epi.17613.

Tekturk, P., Erdogan, E.T., Kurt, A., Kocagoncu, E., Kucuk, Z., Kinay, D., et al., 2016. Transcranial direct current stimulation improves seizure control in patients with Rasmussen encephalitis. Epileptic Disord. 18, 58–66. https://doi.org/10.1684/epd.2016.0796.

Tong, X., Wang, J., Qin, L., Zhou, J., Guan, Y., Zhai, F., et al., 2022. Analysis of power spectrum and phase lag index changes following deep brain stimulation of the anterior nucleus of the thalamus in patients with drug-resistant epilepsy: A retrospective study. Seizure 96, 6–12. https://doi.org/10.1016/j.seizure.2022.01.004.

Van Veen, B.D., Van Drongelen, W., Yuchtman, M., Suzuki, A., 1997. Localization of brain electrical activity via linearly constrained minimum variance spatial filtering. IEEE Trans Biomed Eng 44, 867–880. https://doi.org/10.1109/10.623056.

Wang, H.E., Scholly, J., Triebkorn, P., Sip, V., Medina Villalon, S., Woodman, M.M., et al., 2021. VEP atlas: An anatomic and functional human brain atlas dedicated to epilepsy patients. J Neurosci Methods 348, 108983. https://doi.org/10.1016/j.jneumeth.2020.108983.

Yang, D., Wang, Q., Xu, C., Fang, F., Fan, J., Li, L., et al., 2020. Transcranial direct current stimulation reduces seizure frequency in patients with refractory focal epilepsy: A randomized, double-blind, sham-controlled, and three-arm parallel multicenter study. Brain Stimul. 13, 109–116. https://doi.org/10.1016/j.brs.2019.09.006.